JPET Fast Forward. Published on December 27, 2018 as DOI: 10.1124/jpet.118.254672
This article has not been copyedited and formatted. The final version may differ from this version.

CNS Delivery and Anti-Inflammatory Effects of Intranasally Administered Cyclosporine-A in Cationic Nanoformulations

Sunita Yadav[1,3], Grishma Pawar[1], Praveen Kulkarni[2], Craig Ferris[1,2], and Mansoor Amiji[1,4]

[1]Department of Pharmaceutical Sciences, School of Pharmacy
Northeastern University, Boston, MA 02115 USA
[2]Center for Translational Neuro-Imaging, Northeastern University,
Boston, MA 02115 USA
[3]Novartis Institute of Biomedical Research, Cambridge, MA 02142 USA

Running title page

Running title:" Intranasal CSA in Nanoemulsion".

Corresponding author:
Mansoor Amiji
Northeastern University
360 Huntington Avenue – 140 TF
Boston, MA - 02115
Tel. (617) 373-3137
Fax (617) 373-8886
Email: m.amiji@northeastern.edu

Number of text pages: 47
Number of tables: 1
Number of figures:6
Number of references: 21
Number of words in abstract: 192
Number of words in Introduction: 640
Number of words in discussion: 1004

Abbreviations:

AB – Apical to basolateral
BA – basolateral to apical
BBB – blood brain barrier
CNS – central nervous system
CSA – Cyclosporine A
CSA-NE – positively charged CSA nanoemulsion
LPS – lipopolysaccharide
MRI – Magnetic resonance imaging
NE-SA – positively charged CSA nanoemulsion
NE-T – negatively charged CSA nanoemulsion
T-CSA - CSA solution in 0.5% dimethylsulfoxide HBSS 1X buffer
CSA-S – Aqueous suspension of CSA
TNF-α – Tumor Necrosis Factor-Alpha

ABSTRACT

The main objective of this study was to develop and evaluate the CNS delivery efficiency, distribution, therapeutic efficacy, and safety of cyclosporine-A (CSA) using cationic oil-in-water nanoemulsion system upon intranasal administration. Omega-3 fatty acid rich flaxseed oil-based nanoemulsion was utilized for intranasal delivery to brain and further magnetic resonance imaging (MRI) was used to evaluate and confirm transport of the CSA nanoemulsion (CSA-NE) in CNS. Furthermore, the anti-inflammatory potential of CSA peptide was evaluated using the lipopolysaccharide (LPS) model of neuroinflammation in rats. CSA-NE showed a good safety profile when tested *in vitro* in RPMI 2650 cells. Upon intranasal administration in rats, nanoemulsion delivery system showed higher uptake in major regions of brain when dosed intranasally based on changes in the MR T_1 relaxivity values. Additionally, CSA nanoemulsion showed improved therapeutic efficacy by inhibiting proinflammatory cytokines in the LPS stimulated rat model of neuroinflammation as compared to solution formulation. Preliminary safety evaluations show that the nanoemulsion system was well tolerated and did not cause any acute negative effects in rats. Based on these results, intranasal delivery of CSA and other “neuroprotective peptides” may provide a clinically translatable strategy for treating neurological diseases.

***Keywords*:** CNS delivery, blood-brain barrier, intranasal administration, cyclosporine-A, nanoemulsion, anti-inflammatory

INTRODUCTION

Various neurological conditions, such as neuroinflammation, pain, psychiatric disorders, stroke, and brain cancers can benefit significantly from disease modifying biological therapies such as peptides and proteins (Yi, Manickam et al. 2014). However, due to their inherent instability, large molecular weight, and permeability restrictions these molecules are unable to cross the blood-brain barrier (BBB) upon systemic administration. (Yi, Manickam et al. 2014). Additionally, these molecules have rapid clearance and short half-life in the systemic circulation (Yi et al., 2014). While several strategies are available that include neurosurgical-based delivery such as intraventricular drug infusion, intracerebral implants, hyperosmotic opening of the BBB, and convection enhanced delivery to brain, most of these strategies are highly invasive and risky strategies (Lu et al., 2014).

Cyclosporine-A (CSA), a cyclic decapeptide, a potent immunosuppressive agent that has shown great potential as a neuroprotective agent (Osman, 2014). Due to its immunosuppressant properties of altering T-lymphocytes (inhibition of interlukin production in T cells) activity, it has been utilized in transplant medicine and has also been used to reduce the incidence of transplant rejection (Osman et al., 2011). CSA has also been known to play an important role as neuroprotective agent by preventing MPTP (mitochondrial permeability transition pore) and thus helps in preserving normal mitochondrial function, which can prevent strokes (Osman et al., 2011). Various in vitro and in vivo studies have demonstrated that CSA plays a role in preventing neuronal

damage in models of excitotoxicity and also helps in regulation of neurotransmitter release. (Solomon H. Snyder, 1998; Schauwecker, 2003). CSA has also shown neuroprotective effects in various neurodegenerative diseases by inducing production of certain neurotrophic factors (Bozena Gabryel, 2008) (K Miyata, 2001; Jason Sheehan, 2006).

However, such beneficial effects of CSA were only observed by chronic administration of the drug at a very high dose of >10mg/kg. The higher dosing strategy leads to systemic levels of CSA that produce limiting negative side effects, such as immune suppression, hepatotoxicity, and nephrotoxicity (Patrick, 1996; Osman et al., 2011). Hence, CSA as a potential neurotherapeutic has not been explored so far. Given the above obstacles in utilizing CSA as a neuroprotective agent, there has been an increased interest in developing alternative strategies for delivering CSA specifically to the brain and limiting systemic exposure.

This study was aimed at delivering CSA to the brain using the intranasal route to enhance the therapeutic anti-inflammatory effects with decreased dose and dose related side effects. Intranasal route was utilized for CSA brain delivery as it a non-invasive route of administration and takes advantage of the olfactory epithelium for brain drug delivery without any systemic exposure. Intranasal delivery since its discovery has been utilized in rats (Chow et al., 2001), in animal models of Alzheimer's disease (Jogani et al., 2008), brain tumors (Hashizume et al., 2008), epilepsy (Barakat et al., 2006) and pain (Westin et al., 2005). Intranasal administration has also been used in few human studies (Benedict et al., 2004; Foltin and Haney, 2004; Kosfeld et al., 2005)

for delivering certain biological molecules. Most of the intranasal studies have been focused on efficacy of therapeutic molecules and less is known about how various formulations and molecules get distributed in brain upon intranasal dosing (Per G Djupesland, 2014). Recently, different imaging techniques have been utilized in the diagnosis of brain diseases. We have utilized magnetic resonance imaging (MRI) as a non-invasive way of characterizing the transport of the delivery system in different regions of brain upon intranasal administration. Secondly, an omega 3-rich polyunsaturated fatty acid (PUFA)-based nanoemulsion formulation was developed for effective encapsulation of this peptide to overcome absorption limitation within the nasal cavity and for enhancing nose to brain delivery. Nanoemulsions are oil-in-water or water-in-oil formulations which can be prepared with various edible oils and they are versatile in the types of payloads and targeting capabilities that can be made possible (Singh et al., 2017).

MATERIALS AND METHODS

Statistical Analysis:

The primary statistical analysis was done using GraphPad Prism (version 7.00, La Jolla California, USA, www.graphpad.com).

The *in vitro* transfection studies in LPS model were analyzed using One-Way ANOVA (Tukey's multiple comparison test). The *in vivo* transfection studies in an LPS rodent model of neuroinflammation were analyzed using student *t*-test to compare different treatment groups. For the MRI studies, statistical student's *t* tests were

performed on % change of T1 value for major brain regions and specific 172 brain regions of each subject. The *t*-test statistics using a 95% confidence level (*p<0.05) and 99% (**p<0.001) confidence level, 2-tailed distributions, and heteroscedastic variance assumptions were performed.

1. Materials

High omega-3 fatty acid-containing flaxseed oil was kindly provided by Jedwards International (Quincy, MA). Lipoid E80® was purchased from Lipoid GMBH (Ludwigshafen, Germany). Tween 80®, stearylamine and cyclosporine a peptide was purchased from Sigma Chemicals, Inc. (St. Louis, MO). The nasal septum carcinoma cell line (RPMI 2650) was purchased from American Type Culture Collections (ATCC, Rockville, MD). The media and reagents necessary for culturing RPMI 2650, primers and PCR reagent were purchased from Life Technologies (Invitrogen, Carlsbad, CA). Transwell® companion plates and inserts were purchased from BD Biosciences (San Jose, CA). Gadolinium (III) chloride hexahydrate, diethylenetriamine pentaacetic acid (DTPA), Arsenazo dye, LPS (*Escherichia coli* 0111:B4) were purchased from Sigma Aldrich (St. Louis, MO). All other chemicals were procured from Fisher Scientific (Fair Lawn, NJ) and were used as received.

2. Preparation and Characterization of CSA Nanoemulsions

Oil-in-water nanoemulsions were prepared by the sonication method. Positively charged nanoemulsions were prepared using stearylamine, whereas the negatively charged nanoemulsion were prepared using the same ingredients except without

stearylamine. The negative surface charge on the nanoemulsions was due to egg phosphatidylcholine (Lipoid E80®) and TweenTween-80, which aids by creating poly(ethylene glycol) surface modification. CSA was dissolved in ethanol (50 mg/ml) to prepare a CSA stock solution. The oil phase was prepared by mixing flax seed oil with the drug in ethanol. The aqueous phase was prepared by using egg phosphatidylcholine (PE) (Lipoid E80®) and TweenTween 80. In case of positively charged nanoemulsions, stearylamine was also added to the aqueous phase. The oil phase (oil-drug mixture) was vortexed for few mins and ethanol was completely evaporated using liquid nitrogen. The oil phase was then added slowly to the aqueous phase containing lipoid E80 and Tween 80 with or without stearylamine. After adding oil phase to the aqueous phase the mixture was homogenized and then ultrasonicated in an ice bath to prevent the sample from excessive heating and to protect the peptide from degradation. As CSA has limited solubiluty in water, an aqueous suspension formulation of CSA was formulated an an appropriate control for CSA nanoemusions. The aqueous suspension of CSA (CSA-S) was prepared by mixing CSA in ethanol with egg phosphatidylcholine in distilled water. Tween 80 was added to the mixture in the same proportion as nanoemusion formulation. A screen was performed to select a correct type and percentage of surfactants/excipients (Tween 80, deoxycholic acid, L-histidine, stearylamine) for the nanoemulsion formulation, with the goal of achieving particle size of less than 250 nm with low polydispersity.

Nanoemulsion formulations were characterized for particle size with use of dynamic light scattering on Brookhaven Instrument's 90 Plus ZetaPALS particle size

analyzer (Holtsville, NY) at a 90˚fixed angle and at 25°C. Nanoemulsions were diluted with de-ionized water and the z-average of oil droplet hydrodynamic diameter as well as the polydispersity index (PDI) were recorded. During the measurement average particle count rate was maintained between 50 and 500 kcps. The ZetaPALS instrument was also used to measure the surface charge (zeta potential) of the nanoemulsions. Measurements were made on diluted nanoemulsions as described above. The refractive index of the nanoemulsion was at 1.33, and the viscosity at 1.0 cps to mimic the values for pure water.

Drug loading, encapsulation efficiency and stability were evaluated using HPLC method. The extent of loading of CSA nanoemulsions (amount of peptide incorporated in internal oil phase of nanoemulsion) was determined using high performance liquid chromatography (HPLC). CSA-nanoemulsion was diluted with 100% Methanol and 50 ul of the dissolved nanoemulsion was injected in HPLC. Mobile phase A (1% trifluoroacetic acid (TFA) in water) and mobile phase B (1% TFA in acetonitrile) were pumped through the Agilent Zorbax 300SB-C18 column (C18, particle size 3.5µm, 4.6mm × 100mm) at a flow rate of 1 mL/min. A gradient of 30% B to 100% B was achieved in 8 mins and peptide elution was monitored at a wavelength of 215 nm. For encapsulation efficiency, 0.5 ml of diluted (100x) formulation was transferred to PVDF Ultra-free centrifugal filter units having 0.1 micron pore size (UFC40VV25, Millipore, Bedford, MA) and centrifuged at 5,000g for 15 min at 4°C. The aqueous phase that moved through the filter into the sample recovery chamber was injected on the HPLC and the concentration of the

peptide was estimated. Encapsulation efficiency was calculated based on mass balance. Nanoemulsions samples were studied for stability with respect to its uniformity (appearance), particle size and surface charge at 3 months after storage at 4°C. Drug loaded nanoemulsions were tested for chemical stability up to 3 months after storage at 4°C.

3. Permeability, Intracellular Uptake, and Cytotoxicity Evaluation in RPMI 2650 Cells

In vitro studies were perfomed to understand the mechanistic aspects of nasal absorption/permeability. The aim was to understand the permeability of CSA nanoemulsions in comparision to solution form through nasal epithelial cells before performing the *in vivo* studies. We have evaluated a number of different *in vitro* nasal permeability models to determine the barrier properties of the nasal mucosa for efficient delivery. RPMI 2650 nasal epithelial cells were selected for the studies as it is the most commonly used human cell line for nasal drug transport studies and originates from an anaplastic squamous cell carcinoma of the nasal septum (Bai et al., 2008). These cells also displayed consistent growth, high stability throughout continued culturing *in vitro*, higher trans-epithelial electrical resistance (TEER) values at air-liquid interface, reproducibility of results and ease of both access and maintenance (Moore and Sandberg, 1964). Furthermore, these cells are also known to form interconnected tight junction proteins ZO-1, occluding, claudin-1 and E-cadherin (Bai et al., 2008).

JPET Fast Forward. Published on December 27, 2018 as DOI: 10.1124/jpet.118.254672
This article has not been copyedited and formatted. The final version may differ from this version.

For the permeability studies, RPMI 2650 cells were cultured on inserts in flat bottomed 12-well plates at a density of 300,000 cells/cm^2. Media was changed every third day until 7 days. The cells were then grown on the air-liquid interface for another 7 days. The TEER value was measured after 14 days and the cells were treated with 20 μM of either positively (NE-SA) or negatively (NE-T) charged CSA nanoemulsions and with CSA solution in 0.5% DMSO HBSS 1X buffer (T-CSA) at similar concentrations (n=3). Permeability of CSA formulations was assesed from apical to basolateral direction (AB) and vice versa at 37°C for 2 h with shaking at 50 rpm. The samples were quantitated by LC-MS/MS method.

In order to evaluate and compare the intracellular uptake of CSA nanoemulsions and CSA in solution, RPMI 2650 cells were cultured on 6 well plates at a density of 300,000 cells/cm^2. Media was changed the next day before treating cells with 20 μM of either positively (NE-SA) or negatively (NE-T) charged CSA nanoemulsions and with CSA solution (T-CSA) in 0.5% DMSO HBSS 1X buffer (n=3). After 3 and 24h of incubation, cells in each well were washed 3 times with cold 1x PBS (pH 7.4) and were lysed using cell lysis buffer. CSA was extracted from the cell lysate using solvent extraction method. Briefly, 500 μl of acetonitrile was added and after mixing cell debris was collected, centrifuged and 800 μl of supernatant was aliquoted out in new tube and dried by solvent evaporation. Dry sample was re-dispersed with 200 μl of 50/50 of LC-MS media buffer B (5 mM ammonium formate in methanol) and acetonitrile. Samples were run on LTQ LC-MS and quantitation was performed based on the calibriation

curve. The amount of total protein was determined using a BCA protein assay kit (Thermo Scientific). The percentage dose uptake per mg of protein was calculated.

For the cytotoxicity studies, RPMI 2650 cells were seeded at a density of 5000 cells/well in 96 wells. After 72 h cells were rinsed and incubated with 10 μM and 20 μM of CSA in nanoemulsion form either positively (NE-SA) or negatively charged (NE-T) and with CSA solution in 0.5% DMSO HBSS 1X buffer (T-CSA) (n=8). Treatment with cell media was used as a negative control and treatment with branched poly(ethylene imine) (PEI, molecular weight 10kDa), a cationic cytotoxic polymer at 10 μg/ml was used as a positive control. Following 48h of treatment time, the cells were rinsed with media and 50 μl of 5 mM MTT reagent in PBS (pH 7.4) (Vybrant® MTT Cell Proliferation Assay Kit, Life Technologies) was added. During the incubation period of 1h at 37°C, MTT dye was converted to formazan by the live cells. DMSO 200 μl was added to the plates and after shaking for few minutes, the absorbance value was measured at 490nm. In this assay, the absorbance value is directly proportional to the live cells. The percent cell viability was calculated from the absorbance values relative to those of untreated cells.

4. *In Vitro* Evaluation of Anti-inflammatory Effects of CSA Nanoemulsion in LPS-Stimulated Macrophages

To quantitatively assess the potential anti-inflammatory therapeutic effect of the CSA loaded nanoemulsion, the levels of pro-inflammatory cytokines tumor necrosis factor α (TNFα), interleukin-1β (IL-1β), interleukin-6 (IL-6), and the inducible nitric oxide

synthase (iNOS) were measured at the mRNA levels by RT-PCR in LPS (Sigma Aldrich) stimulated J774A.1 macrophages. Cells were counted and plated on day one in a 6-well micro plate at 50,000 cell density and after day 4 cells were first treated with either CSA in aqueous solution (CSA-S) or with CSA nanoemulsion (positively charged nanoemulsion (CSA-NE)) formulation for 4h (n=3) at a concentration of 1 µg/ml. After 4h of pre-treatment, cells were stimulated with 100 ng/ml of LPS. Prior to confirming 100 ng/ml as final LPS dose, several concentrations of LPS at several time points were experimented on cells and 100 ng/ml LPS for 6 h resulted in significant up regulation of target cytokines. Following 6 h of stimulation, cells were washed and collected by centrifugation at 5,000 g for 10 min. Cell pellet was used for RNA extraction using the manufacture protocol (Roche, Indianapolis, IN.). The extracted RNA was quantified and about 400 ng RNA was used for cDNA synthesis (Taqman reverse transcription reagent). The second step qPCR was performed using Taqman probes for specific cytokines using the Taqman gene expression master mix. Beta-actin was used as internal control. Standard curve was also prepared using cDNA from the LPS treated cells. TNFα levels were measured at protein level by using TNFα specific ELISA kit (R & D Systems) (data not shown).

5. Qualitative Brain Distribution of Intranasal Nanoemulsion in Rats using MRI

The purpose of this comparative study was to compare, the uptake of gadolinium (Gd^{3+}) encapsulated-nanoemulsion (Gd^{3+}-NE) and N-methylglucamine salt of the gadolinium complex of diethylenetriamine pentaacetic acid aqueous solution

(Magnevist®) into brain using MRI which is being considered the gold standard in the diagnosis of brain disorders and brain imaging (Lux and Sherry, 2018). Gd^{3+} contrast agent for MRI has unpaired electrons that interact with surrounding water molecules to decrease their longitudinal relaxation time (T_1). MRI can measure T_1 by creating a magnetic field that reverses the sample's magnetization, then recording the time required for the spin directions to realign in their equilibrium positions. A decrease in the T_1 relaxation time from the baseline T_1 value of the target tissue allows MRI instrument to better distinguish contrast from surrounding environment (Lux and Sherry, 2018).

5.1. Synthesis of PE-DTPA-Gd^{3+} Conjugate:

To prepare the nanoemulsion with Gd^{3+} ions for contrast enhancement in MRI, we synthesized and purified phosphatidylethanolamine-DTPA-Gd^{3+} (PE-DTPA-Gd^{3+}) conjugate. To chelate Gd^{3+} ions for MRI contrast, phosphatidylethanolamine (PE) was conjugated with diethylenetriamine pentacetic acid (DTPA) using a previously published protocol (Sandip et al., 2006).

Triethylamine (60 µl) was added to egg phosphatidylethanolamine (200 mg), which was dissolved in 8 ml of chloroform. The solution was then added drop-wise to 1 mM of DTPA anhydride solution (800 mg in 40 ml of DMSO) and the mixture was stirred for 3 h under nitrogen atmosphere in an open flask. The suspension was dialyzed overnight using 2 kDa molecular weight cut off membranes (Spectra/PorSpectrum Labs, CA), to eliminate free DTPA and the resulting conjugate was lyophilized. Gadolinium trichloride (37mg - equivalent to 40.0 mmol) dissolved in 0.2ml of water was added drop

wise to the DTPA-PE mixture (dissolved in 40ml DMSO) and stirred for 1 h, followed by dialysis with water using 2 kDa membrane. The water was changed three times a day. The final DTPA-PE-Gd mixture was lyophilized for 2 to 3 days. Free gadolinium is a known toxin and a heavy metal and may contribute towards total gadolinium concentration. The amount of free gadolinium in the complex was checked using the 200 µl of 0.2 mM Arsenazo dye. Arsenazo III binds to metal ions forming an Arsenazo-metal ion complex, which was qualitatively analyzed by the color change. The final product was stored at -80°C and was used to prepare the formulations

5.2. Formulation of Gd^{3+} Labeled Nanoemulsions for MRI: Gd^{3+}ions containing nanoemulsions were prepared by a high energy ultra-sonication method.. From above DTPA-PE-Gd complex (0.5mmoles Gd^{3+}), Lipoid® E80 (48 mg), Tween 80 (8 mg) and stearylamine (8 mg) were added to water (1.6 ml) and the mixture was stirred for 30 mins to achieve complete dissolution of these excipients. Separately 0.4 g of Flaxseed oil was taken in a glass vial. The two phases were then heated on a hot plate at 70°C for 3-5 mins. The aqueous phase was added to the oil phase and the mixture was sonicated at 21 % amplitude and 50 % duty cycle (Sonics and Materials Inc., Vibra Cell VC 505, Newtown, CT) for 10 min, resulting in the formation of the nanoemulsion. The mean particle hydrodynamic diameter and zeta potential of the nanoemulsions droplets was measured as described in the section 2 with a 200-fold dilution of formulation with distilled water.

Magnetic resonance imaging (MRI) was used to determine the longitudinal

relaxation time (T_1) of the Gd^{3+} containing nanoemulsions. According to the exponential decay function, the magnetization is at T_1 is $(1-\frac{1}{e})$, or approximately 1/3 less than the equilibrium magnetization. Hence, by extrapolating the time at this magnetization, it was possible to determine the T_1 relaxation rate. Nanoemulsion was diluted into Eppendrof tubes and run through a Bruker Biospin Bruker Biospec 7.0T /20-cm bore USR horizontal magnet. Magnevist solution which is used as a control was also diluted and run for *in vitro* T_1 values measurements.

5.3. Experimental Design for MRI Studies: All of the animal experiment discussed here were approved by Northeastern University's Institutional Animal Care and Use Committee. Female Sprague Dawley rats (210–230g) were obtained from Charles River Laboratories (Cambridge, MA) and kept on a 12-h light/dark cycle with *ad libitum* access to food and water. All of the described animal experiments were approved by the Northeastern University Institutional Animal Care and Use Committee. Rats were acclimated to their environment for 2 days before the experiments. All MRI experiments were carried out at room temperature. Experiments were conducted using a Bruker Biospec 7.0T/20-cm USR horizontal magnet (Bruker, Billerica, Massachusetts) and a 20-G/cm magnetic field gradient insert (ID = 12 cm). Radiofrequency signals were sent and received with the quad-coil electronics built into the animal restrainer. The rats (n=6) were administered PE-DTPA-Gd^{3+} containing nanoemulsion formulations at 0.02 mmoles/kg (40 µl of total nanoemulsion or Magnevist solution using the 50 µl Hamilton syringe, 5 µl volume administered in alternative nostrils and total volume administered in

20 mins). Rats were placed in a head restrainer for imaging at various time points after the dosing. Pre-dosing images of the rat's brain regions were also collected for comparison of T_1 values.

5.4. Anatomical MR Scans*:* At the beginning of each imaging session, a high-resolution anatomical data set was collected using the RARE pulse sequence (20 slice; 1 mm; field of vision [FOV] 3.0 cm; 256 × 256; repetition time [TR] 2.5 sec; echo time [TE] 12.4 msec; NEX 3;). Variable TR images were acquired using RARE pulse sequence (TE=12.5 and TR: 460, 900, 1400, 2800, 6000, msec.) Images were acquired with a field of view [FOV] 3 cm^2, data matrix = 128×128×20 slices, thickness = 1 mm. T_1 measurements were computed using ParaVision 5.1 software (Bruker, Billerica, Massachusetts) by fitting absolute signal at particular TR. The T1 map data was collected at 128x128 (X-Y) and 22 slices. Voxel resolution was 0.234 x 0.234 mm in plane and slice thickness of 1.2 mm. Field of view (FOV) was 30 x 30 x 26.4.Isoflurane (2.5 - 3 %) was constantly supplied throughout the imaging session using a nose cone to maintain the respiratory rate between 40 to 60 breaths per minute. During image acquisition respiratory rate was monitored continuously over the entire imaging period using a small animal heating and monitoring system (SA Instruments, Stonybrook, NY). After the first baseline scan (pre-dose scan) of whole brain, rats were administered a total dose of 0.1 mmoles/kg based on body weight. After the dosing was finished within 20 mins, MR scan were commenced to capture post dosing time point of 30 mins, 60 mins, and 90 mins.

5.5. MR Data Analysis and Image Processing: Each subject at different time point 0 min, 30 min, 60 min and 90 min was registered to a 3D segmented and annotated rat brain atlas (Ekam Solutions LLC, Boston MA.). The alignment process was facilitated by an interactive graphic user interface, EVA (http://ekamsolutions.com/). The affine registration involved translation, rotation, and scaling in all 3 dimensions independently. The matrices that transformed the subject's anatomy to the atlas space were used to embed each slice within the atlas. All transformed pixel locations of the anatomy images were tagged with the segmented atlas regions, creating a fully segmented representation of each subject. Each subject is segmented into 172 distinct brain regions. T_1 parameter values for each ROI was computed based on each segmented map**.**

Percent change decrease in T_1 values at each time point and in each major regions and specific regions was calculated at *t* = 30 min, 60 min and 90 min time point as described:

$$\%Change\ in\ T_1 value\ of\ ROI\ at\ t = \frac{(T_1\ of\ ROI\ at\ 0\ min - T_1\ of\ ROI\ at\ t\ min) \times 100}{T_1\ of\ ROI\ at\ time\ 0}$$

6. *In Vivo* Evaluation of Therapeutic Efficacy of CSA Nanoemulsion in an LPS Rat Model of Neuroinflammation

In order to evaluate and compare the protective anti-inflammatory effect of cyclosporine in LPS-induced degeneration of nigral dopaminergic neurons, Sprague Dawley rats were pretreated with 5 mg/kg of CSA in solution (CSA-S) and positively

charged nanoemulsion (CSA-NE) formulation. Rats were briefly anesthetized using ketamine and xylazine (80 and 20 mg/kg respectively) and following sedation rats were dosed with 5 mg/kg of CSA-S and CSA-NE intranasally over a period of 30 mins using a 20 µl manual micropipette. Rats were pre-treated with CSA formulations 3 h prior to the LPS treatment.

For LPS injection, the Sprague Dawley rats were deeply anesthetized using isoflurane (2.5-3 %). The animal's head was shaved and swabbed with 70% isopropyl alcohol and betadine. Rats were then placed in the stereotaxic instrument. Body temperature was maintained throughout the procedure at 38°C using a heating pad (Fintronics). A sterile scalpel was used to create a 1-2 cm rostral to caudal incision on the scalp, and to expose the bregma. Tissue overlying the suture lines was scraped away and the skull was dried using a dryer. A surgical drill (Dremel®) was then used to create a burr hole (1-2 mm) at the following stereotaxic coordinates were used: 4.8 mm posterior to bregma, 1.7 mm lateral to the midline, and 8.2 mm ventral to the surface of the skull (Paxinos and Watson, 1986) for injection into the substantia nigra region. Rats were dosed 2 µg of LPS and cytokine stimulation was evaluated at 6 h time point. The needle of a 5 µl Hamilton syringe, containing the LPS solution, was then lowered -8.8 mm ventral to the surface of the skull and 1 µl of LPS was injected using a motorized microinjection Harvard apparatus infusion pump at a rate of 0.5 µl/min. After the injection, the needle was kept in place for 2 min and then slowly pulled out to minimize efflux. LPS was prepared as a stock solution of 2 mg/ml in sterile PBS (pH 7.4). Each rat received an injection of LPS dissolved in PBS onto the right side of brain and the

contralateral left side was used as an internal control and was analyzed separately. After LPS injection rats were returned to cage and food and water was supplied. After 6 hrs post-LPS injection, the rats were sacrificed, and brain was dissected. Micro dissection was performed using the adult rat brain slicer matrix and 1-2 mm of the slices were dissected. Substantia nigral (SN) region from both injected side and contralateral side was collected and was frozen immediately. Tissues samples were processed further after homogenization with Qiazol™ (Invitrogen) to perform RNA extraction. Total RNA was isolated and purified from brain tissue using RNA-Easy Lipid Tissue Mini Kit as per instructions from Qiagen (Maryland, USA). The isolated mRNA from the tissue samples described above was quantified by UV spectrophotometry using the Nano-Drop Instrument (Thermo Fisher Corp.). Gene quantitation assay using TaqMan gene expression master mix and TaqMan gene expression assays from Applied Biosystems (Foster, CA) was performed as per instructions. The samples were run in triplicates and data was analyzed using comparative threshold cycle (Ct) method by calculating $\Delta\Delta$Ct values for each treatment and results were expressed as % relative expression compared to β-actin as endogenous control and normalized to the untreated animals.

7. Acute Safety Assessments

To examine the safety, following study was designed for each treatment groups as solution and as nanoemulsion with controls: body weight monitoring, histopathological evaluation of nasal mucosa and histopathological evaluation of liver sections.

7.1. Changes in Body Weight: Periodic measurements of the body weight were performed upon injecting the control (PBS only), CSA-S (5 mg/kg) and CSA-NE (5 mg/kg) formulation via intranasal route of administration on day 0 to day 3. Frequent body weight measurements were made through the course of the study. A total of two animals were used. The results were plotted as percent change in body weight as a function of day's pre-treatment administration for all the treatment groups.

7.2. Nasal Tissue Histopathology: To evaluate the toxic effect on the nasal mucosa, rats were first dosed with 5 mg/kg of CSA-S and CSA-NE and only saline was used as a control. After exsanguination at 6 hour time point post administration, the head was removed from the carcasses. The tissues samples were preserved in formalin fixative until histopathological processing. After fixation and decalcification, four tissue slices were taken at the following levels: 1) Immediately posterior to the upper incisor teeth 2). At the incisive papilla or the anterior nasal cavity 3). Premolar or middle part of the nasal cavity 4). At the middle of the first molar teeth or posterior part of the nasal cavity. The nasal tissues were processed in a conventional manner. Paraffin embedded tissues were cut into 5 µm sections and mounted on a glass slides and cover slips were placed on glass slides. Tissue sections were dried and de-paraffinized using xylene substitute followed by decreasing concentrations of ethanol down to purified water. Sections were incubated in hematoxylin, rinsed with water, and incubated with 1% acid alcohol (clearing reagent). Sections were rinsed and incubated with 4% ammonia solution (bluing reagent). Sections were then incubated with Eosin followed by dehydration by two changes each in 95% ethanol and 100% ethanol followed by final

change of xylene substitute. Tissues were then mounted on slide and cover slips were placed on glass slides and digital image was captured using a light microscopy (n=2 / treatment). Blinded analysis oftoxicological profile and tissue damage, if any, was carried out by Dr. Jerry Lyon, a certified veterinary pathologist, at the Tufts University Veterinary School in Grafton, MA.

7.3. Liver Tissue Histopathology*:* Liver tissues samples were collected for histopathological analysis from rats after 3 days of post treatment with PBS (control) , 5 mg/kg of CSA-S and CSA-NE formulations via intranasal route of administration. These tissue samples were preserved in formalin before analysis. Paraffin embedded tissues were microtomed into 5 µm sections and mounted on glass slides and a cover slip was placed on top of the tissue sample in eachslide. The tissue sections were dried and de-paraffinized using xylene substitute followed by decreasing concentrations of ethanol to down to purified water. Sections were incubated in hematoxylin, rinsed with water, and incubated with 1% acid alcohol (clearing reagent). Sections were rinsed and incubated with 4% ammonia solution (bluing reagent). Sections were then incubated with Eosin followed by dehydration by two changes each in 95% ethanol and 100% ethanol followed by final change of xylene substitute. Tissues were mounted on slide and digital image was captured using a light microscopy. Blinded analysis of toxicological profile and tissue damage, if any, was carried out by Dr. Jerry Lyon, a certified veterinary pathologist, at the Tufts University Veterinary School in Grafton, MA.

RESULTS

1. Preparation and Characterization of CSA Nanoemulsions

The final composition that showed the best particle size distribution for nanomeulsion was found to be 2.5% w/v lipoid E80, 0.2% w/v Tween 80, 0.2% w/v stearylamine and 20% w/v flax-seed oil **(Table 1).** The theoretical loadings for positive and negative nanoemulsions were different as CSA had different solubility profile with and without stearylamine. Both negative and positive charged formulations were used for comparison in cell transport and tolerability studies.

2. Permeability, Intracellular Uptake, and Cytotoxicity Evaluation

We were able to utilize the RPMI 2650 cells for transport studies as it formed a uniform confluent monolayer when cells were grown under an air-liquid interface. Highest TEER values of 200 Ohm/cm^2 were observed when cells were seeded at a density of 4 x 10^5 cells/cm^2 onto a PET insert of 0.4cm^2 surface area with 0.4 µm pore size, which demonstrates the barrier-like properties of the model. RPMI 2650 cells also showed the presence of the tight junction protein Z0-1 (data not shown). Furthermore, the apparent permeability coefficient of the paracellular marker sodium fluorescein was found to be (8.07±0.01) x10^{-6} cm/s, which is indication of uniform monolayer (Wengst and Reichl, 2010; Goncalves et al., 2016). RPMI 2650 cell monolayer was used to assess and compare the transport of the CSA peptide formulations. The delivery of CSA via positively charged nanoemulsion formulation showed increase in apical to basolateral transport (582 ± 5 ng/ml) when compared to transport of CSA solution (100 ± 20 ng/ml) (**Figure 1A)**. Negatively charged nanoemulsion was unable to show increase in transport of CSA. These findings indicating increase in transport of CSA via

positively charged nanoemulsion formulation with simultaneous decrease in the efflux are of immense importance since CSA is an efflux substrate. Intracellular studies performed with CSA peptide showed no major difference between solution or nanoemulsion formulations for the early time point of 3 h. However, nanoemulsion at a later time point of 24 hrs showed increase in uptake but the T-CSA solution showed decrease over time. Nanoemulsion showed potential for enhanced uptake in cells at later time point and uptake seems to not saturate overtime. There was no clear difference for intracellular uptake for NE-SA (positively charged) and NE-T formulation (negatively charged) formulations (**Figure 1B).**

CSA nanoemulsion formulations with positive and negative charged showed enhanced tolerability up to a concentration of 20 μM as compared to the solution form of the peptide which showed viability of only 75% under similar conditions (**Figure 1C**). This shows that the CSA nanoemulsions are less cytotoxic as compared to solution form of CSA. As positively charged nanoemulsion showed overall enhanced cell transport, this formulation was selected for further comparative studies and was labeled as NE-SA for all further studies.

3. Anti-Inflammatory Effects of CSA in LPS-Stimulated Macrophages

The potential anti-inflammatory effect of CSA-NE (positively charged nanoemulsions) in J774A.1 macrophages was evaluated by measuring the levels of TNFα, IL-1β, IL-6 and iNOS proinflammatory cytokines, following stimulation with LPS toxin. Firstly, we determined the cytokines, which showed stimulation with LPS.

Previously, we have seen that stimulation of cells with LPS for 4 to 6 h time point results in high stimulation of these cytokines (Jain and Amiji, 2012). We selected 4 hour as a pre-treatment time point for the CSA nanoemulsion (CSA-NE) and aqueous CSA solution (CSA-S). All four cytokines standard curves were found to be linear with a good slope value (Data not shown). When comparing the aqueous solution of CSA to NE formulation (1 µg/ml), there was a significant decrease in the mRNA levels of all four cytokines **(Figure 2).** Data was plotted by considering the expression of specific marker as 100% in untreated cells that were not given any treatment. Solution formulation at this concentration tested showed less of an effect on the cytokines possibly due to the reduced uptake and high efflux of CSA solution, which was evident in the transport studies performed with nasal squamous epithelial cells.

4. Transport of Gd^{3+}-Labeled Nanoemulsion using MRI

PE-DTPA-Gd^{3+} complex formed was found to be free of any gadolinium ions when tested with Arsenazo dye. These complexes were further used in the nanoemulsions where the PE-DTPA-Gd^{3+} complex was integrated into the nanoemulsion layer and Gd^{3+} ion on the surface served as the contrast agent for the MR imaging studies *in vivo* **(Supplementary Figure 1)**. Particle size characterization showed the z-average to be 342.4 ± 21nm with a PDI of 0.20 and a surface charge of 26.5 mV ± 0.833 mV. PE-DTPA-Gd^{3+} ion-containing nanoemulsions were also characterized using *in vitro* magnetic relaxivity values. (**Supplementary Figure 2)** relates concentration of Gd^{3+} with the reciprocal of T_1, a relation that results in a linear

line with a slope of 6.58 sec^{-1} $mmole^{-1}$. This slope is referred to as R_1 or the magnetic relaxivity and indicated the relative contrast efficiency. The R_1 values of the Gd^{3+}-NE were compared to Magnevist® solution, which is a commercially marketed contrast agent and served here as the standard basis for comparison. It is clear from **Supplementary Figure 2** that Gd^{3+}-NE significantly reduced the relaxation time relative to pure water and had a higher slope (meaning grater R_1 value) as compared to that of Magnevist®.

The results in **Figure 3A** show the anterior to posterior overlay of rat's brain regions, which showed significant changes in T_1 values upon Gd^{3+}-NE intranasal delivery. MRI studies of the different major regions of brain following intranasal administration of Gd^{3+}-NE resulted in a unique and widespread distribution of Gd^{3+}-NE in brain as is evident by the significant decrease in T_1 values in the major regions of brain **(Figure 3B).** There was a fast uptake within the first 30 mins as observed by a significant T_1 value drop in most of the regions of the brain except the cerebellum and amygdaloidal. This drop in T_1 value was found to be significant when compared to the control group. In the cerebellum, including in the cranial nerves and ventral striatum, there was a significant difference in the relaxivity values at 55-60 mins post-administration (**Figure 3C**). When the data was analyzed for the 172 specific regions of brain, we found 22 brain regions out of 172 regions showing higher and significant uptake for the Gd^{3+}-NE compared to control **(Figure 4)**. Magnevist® distribution in brain was found to be lower than the Gd^{3+}-NE distribution (as evident from the higher decrease in T_1 changes due to Gd^{3+}-NE) suggesting a possibility that nanoemulsion are

being taken up by intracellular endocytosis process or through the trigeminal pathways where they could lead to higher uptake in different and distant regions of brain. Further, nanoemulsion shows signal in different regions of brain for a longer time period as compared to Gd in solution (i.e., Magnevist®).

5. Evaluations, of the Anti-Inflammatory Effects of CSA-NE in an LPS Rat Model of Neuroinflammation

We utilized the LPS-induced model and performed qPCR analysis to evaluate the cytokines profile in substantial nigra (SN) regions upon treatment with control and nanoemulsion formulation for CSA. Both the injectable site SN and contralateral side SN were dissected from brain after 6 h post-LPS injection. Samples were then processed for total RNA extraction, cDNA synthesis and subsequent PCR amplification. From **Figure 5** it can be seen that the percentage relative cytokine levels for different treatment groups after 3 h of pre-treatment with CSA. As indicated in the figure, the levels of pro-inflammatory cytokines for the LPS-induced rats on the right side of substantia nigra (LPS only R) were found to be significantly higher than the non-LPS control saline group (control saline R). For instance, the percent relative expression of TNFα, iNOS, IL-6 after LPS stimulation was found to be 19,177 +/- 269%, 1,876 +/- 725%, and 2,300 +/- 576%. CSA delivered as solution formulation was found to be slightly effective in exerting therapeutic effect at this time point, where TNFα reached 14,223 +/- 7305%, with higher variability within the levels. The considerably lower effect of the CSA-solution was also found in the *in vitro* studies conducted in LPS-stimulated

macrophages. On the other hand, CSA-NE significantly lowered the levels of TNFα (2,786 +/- 328%) compared to the LPS-induced group and compared to the CSA solution group which emphasizes the importance of a nanomeulsion based delivery system. The levels of other cytokines IL-2 and IL-6 were also found to be lowered however; the results were not significantly different. IL-2 is another cytokine specifically down regulated by CSA and has been studied to be upregulated by T lymphocytes. Upon LPS stimulation, apart from microglia there is evidence that lymphocytes can also infiltrate the injection site**.** CSA-NE showed inhibition of the IL-2 gene expression which is known to be involved in the maintenance of regulatory T cells and is also involved in the differentiation plus survival of T cells. The therapeutic effects observed on IL-2 cytokine were based on the inhibition of the endogenous levels. It was later found that LPS is not an effective stimulator of IL-2 levels and hence if the levels of IL-2 are considerably increased using other types of toxin we might be able to observe a higher inhibition effect on this cytokine. Overall, CSA-NE treatment was found to be considerably effective in inhibiting the expression of cytokines including TNFα and was found to be slightly effective in down regulating other cytokines like IL-2 and IL-6 though not significant. There was no effect of CSA-NE or CSA-S on iNOS levels.

6. Acute Safety Assessments

There was a slight difference in the body weights of rats treated with the three groups: PBS control, CSA-S, and CSA-NE. After day 1, all the groups gained weight except CSA-S group. Rats in CSA-NE group showed a steady gain in weight after day 1

(**Figure 6A**). These results suggest that the nanoemulsion formulation were well tolerated in rats.

Based on the histopathological report, all the normal structures of the nasal cavities were identified, and no significant pathology is identified in any of the sections for any of the animals. Upon a closer view of the respiratory and the olfactory mucosal lining of the nasal cavity, there were no significant changes in both the epithelial cell lining the nasal cavity **(Figure 6B).** As shown in (**Figure 6C)**, there was moderate periacinar and diffused hepatocellular vacuolation. Occasional multifocal aggregates of cells were present in portal areas consistent with extra-medullary hematopoiesis (Li et al., 2003). Mild extra-medullary hematopoiesis and lipid vacuolation are considered as common incidental findings in the liver and are not thought to be related to the treatment as they were also observed in control naive animals (R24) (Li et al., 2003). Hence, the liver tissues histopathological findings for treated groups are consistent with what is regarded as within normal limits.

DISCUSSION

Peptides have been investigated as potential agents for the treatment of various CNS disorders. There is an unmet need for therapeutic strategies to ensure the efficient delivery of peptide drugs to the brain(Yi et al., 2014). Recently, intranasal delivery has gained lot of attention for direct delivery of drugs to brain and CNS (Per G Djupesland, 2014). In the previous study we have shown that nanomeulsion of Cyclosporine are capable of showing higher brain targeting upon intranasal delivery (Yadav et al., 2015).

Nanoemulsion when compared to solution formulation showed enhanced uptake in different regions of brain with lower systemic exposure upon intranasal administration (Yadav et al., 2015). This study was designed to further evaluate and understand the benefits of using nanoemulsion delivery system for intranasal delivery of CSA peptide to brain. We discussed few limiting factors of nasal absorption in the introduction section like physical barrier or poor permeability of large molecular weight drugs, enzymatic barrier of nasal mucosa, efflux transporters etc. *In vitro* models of nasal mucosa have been utilized using excised tissues, primary cell cultures or immortalized cell lines (Wengst and Reichl, 2010). However, excised human tissue is hard to obtain and using animal tissues introduces high variability in addition to question regarding species differences. Hence, in an attempt to understand the barriers for CSA nasal administration, we utilized the RPMI 2650 cell model to study the cell transport and found that positively charged CSA-NE showed higher cell transport from apical to basolateral (AB) direction. Also the transport from basolateral to apical (BA) direction was reduced which signifies reduction in efflux of CSA. Furthermore, increase in intracellular uptake was found for CSA-NE formulations especially at later time which further confirms that cyclosporine transport through efflux transporter is reduced by using oil-in-water nanoemulsion particulate system.

CSA-NE system were found to be well tolerated in the murine macrophage cells and hence considered safe to be used further for *in vivo* evaluations. To understand the benefit of nanomeulsion formulations we further compared the anti-inflammatory effect of CSA in J774A.1 macrophages, which were stimulated by LPS. These cells were used

as surrogate cell model due to limited supply/source of primary microglia. Bacterial LPS has been extensively used in models studying inflammation as it mimics many inflammatory effects of cytokines, such as up regulation of cytokines like TNFα, IL-1β or IL-6. LPS is the most abundant component within the cell wall of Gram-negative bacteria. It can stimulate the release of inflammatory cytokines in various cell types, leading to an acute inflammatory response towards pathogens (Abe et al., 1995). When tested in J774A.1 cells, CSA-NE showed reduction in cytokine stimulation upon LPS stimulation, which is most likely due to higher transport and intracellular concentration of CSA when compared to CSA-S. Nanoemulsion overall showed benefits over solution of CSA due to their potential in avoiding efflux which in turn leads to high intracellular accumulation compared to solution form of the peptide. Due to their positive inhibitory effect on the various cytokines, we further evaluated these formulations *in vivo* in an LPS stimulated neuroinflammation model.

Furthermore, to assess and understand the potential advantages of using nanocarrier based system rather than aqueous formulations for intranasal delivery to brain, we designed MRI based uptake study. Based on the distribution study, we demonstrated that Gd^{3+} ion containing nanoemulsion can reach multiple sites within the brain as early as 30 mins after the intranasal administration. In some brain regions there was a significant change in T_1 values of up to 10 to 15%. It is evident that some of the areas where higher T_1 changes were observed are not in close proximity of olfactory bulbs. The wide distribution of CSA in brain can be attributed to the olfactory neuronal pathway and trigeminal nerve pathway (Mittal et al., 2014). The distribution of CSA from

olfactory bulbs to other parts of the brain as observed from MRI can be attributed to diffusion that can also be driven by perivascular pump. This could be driven by arterial pulsation in the brain (Mittal et al., 2014)..Furthermore, the distribution and uptake was found to be significantly different then the uptake of Magnevist® aqueous solution. This potentially is due to low residence time of aqueous solutions into the nasal cavity and hence less chance for nasal absorption by the olfactory epithelium due to rapid clearance via mucociliary clearance mechanism. We have demonstrated that intranasal application of Gd^{3+}-NE results in rapid delivery to multiple regions of CNS, which are known to be involved in the pathogenesis of neurodegenerative diseases.

For the therapeutic benefit of CSA in the brain, we tested these formulations *in vivo* in a rat LPS model of neuroinflammation. The amount of LPS used has previously been reported to cause stimulation of various cytokines together with damage to nigral dopaminergic neurons and astrocytes *in vivo* (Liu et al., 2000; Tomás-Camardiel et al., 2004). Our therapeutic efficacy studies conducted in LPS-induced model of neuroinflammation showed intranasal delivery of nanoemulsion incorporating anti-inflammatory molecule like cyclosporine was capable of inhibiting the activated cytokines to greater extent over the solution formulation treatments. The better effect observed with nanoemulsion again highlights the importance of using nanoemulsion which have shown better brain targeting efficiency based on the distribution study performed earlier (Yadav et al., 2015). The deleterious role of activated microglia together with mediators (cytokines, complement factors) under conditions of inflammation in the CNS is becoming more evident and are found to be closely

associated to degenerating neurons (McGeer and McGeer, 1995). The therapeutic approach of using anti-inflammatory measures for targeted delivery to CNS could really be beneficial for slow progressing diseases of the brain, which are associated with inflammation.

In addition to evaluating delivery and therapeutic efficacy, it was of utmost importance to monitor the safety and tolerability of formulations delivered through the intranasal route. As local toxicity to the nasal mucosa will be detrimental, we looked into the impact of using nanoemulsion formulations on nasal tissues along with liver tissues. Our safety results showed no major tolerability problems for intranasal dosing of nanoemulsion.

CONCLUSIONS

Peptide delivery to brain has been a major challenge due to various barriers. We have utilized the intranasal delivery route to directly deliver peptide to brain overcoming the systemic circulation. We have shown efficient delivery of anti-inflammatory peptide (CSA) using cationic nanoemulsion. We showed significant inhibition of pro-inflammatory cytokines both *in vitro* and *in vivo* in the LPS stimulated model of neuroinflammation. Further, nanoemulsion showed enhanced uptake in various regions of brain upon intranasal delivery when compared to solution formulation. Nanoemulsion formulations were found to be safe based on acute safety studies performed in rats. Our results indicate that nanoemulsion enhances nose to brain uptake of peptide and further

are capable of providing therapeutic effects. Further studies considering into the behavioral impact of anti-inflammatory effect when delivered via intranasal route would warranty its clinical usefulness as a non-invasive therapeutic approach for neuroinflammation, a common denominator in many different types of chronic neurodegenerative diseases.

ACKNOWLEDGEMENTS

This study was partially supported by the National Institute of Neurological Disorders and Stroke of the National Institutes of Health through a grant R21-NS066984. We also deeply appreciate the assistance of Dr. Barbara Caldarone and Paul Lorello at Harvard Medical School's Neuro-Discovery Center in Boston for providing training in stereotaxic apparatus use and surgery for microinjection in rats. Dr. Jerry Lyon at the Tufts University's Veterinary School is deeply appreciated for his assistance with the tissue histology and analysis. We deeply appreciate the assistance of Mr. Srujan Kumar Gandham with the neuroinflammation model development and *in vivo* experiments.

AUTHORSHIP CONTRIBUTIONS

Participated in research design: Yadav, Kulkarni, Ferris and Amiji.

Conducted experiments: Yadav and Pawar

Contributed to new agents or analytical tools: Kulkarni, Ferris, and Amiji

Performed data analysis: Yadav, Pawar, and Kulkarni

Wrote or contributed to writing of manuscript: Yadav, Pawar, and Amiji.

REFERENCES

Abe K, Irie T and Uekama K (1995) Enhanced nasal delivery of luteinizing hormone releasing hormone agonist buserelin by oleic acid solubilized and stabilized in hydroxypropyl-beta-cyclodextrin. *ChemPharmBull(Tokyo)* **43**:2232-2237.

Bai S, Yang T, Abbruscato TJ and Ahsan F (2008) Evaluation of human nasal RPMI 2650 cells grown at an air-liquid interface as a model for nasal drug transport studies. *J Pharm Sci* **97**:1165-1178.

Barakat NS, Omar SA and Ahmed AA (2006) Carbamazepine uptake into rat brain following intra-olfactory transport. *J PharmPharmacol* **58**:63-72.

Benedict C, Hallschmid M, Hatke A, Schultes B, Fehm HL, Born J and Kern W (2004) Intranasal insulin improves memory in humans. *Psychoneuroendocrinology* **29**:1326-1334.

Bozena Gabryel JB (2008) Effect of FK506 and cyclosporine A on the expression of BDNF, Tyrosine kinase B and p75 neurotrophin receptors in astrocytes exposed to stimulated ischemia in vitro. *Cell Biology internantional* **33**:739-748.

Chow HH, Anavy N and Villalobos A (2001) Direct nose-brain transport of benzoylecgonine following intranasal administration in rats. *J PharmSci* **90**:1729-1735.

Foltin RW and Haney M (2004) Intranasal cocaine in humans: acute tolerance, cardiovascular and subjective effects. *Pharmacol Biochem Behav* **78**:93-101.

Goncalves VSS, Matias AA, Poejo J, Serra AT and Duarte CMM (2016) Application of RPMI 2650 as a cell model to evaluate solid formulations for intranasal delivery of drugs. *Int J Pharm* **515**:1-10.

Hashizume R, Ozawa T, Gryaznov SM, Bollen AW, Lamborn KR, Frey WH and Deen DF (2008) New therapeutic approach for brain tumors: Intranasal delivery of telomerase inhibitor GRN163. *Neuro Oncol* **10**:112-120.

Jain S and Amiji M (2012) Tuftsin-Modified Alginate Nanoparticles as a Noncondensing Macrophage-Targeted DNA Delivery System. *Biomacromolecules* **13**:1074-1085.

Jason Sheehan MD, PhD., Anne Eischeid, M.S., Randi Saunders, and Nader Pouratian, M.D., PhD. (2006) Potentiation of neurite outgrowth and reduction of apoptosis by immunosuppressive agents: implications for neuronal injury and transplantation. *Neurosurgery focus* **19**.

Jogani VV, Shah PJ, Mishra P, Mishra AK and Misra AR (2008) Intranasal mucoadhesive microemulsion of tacrine to improve brain targeting. *Alzheimer DisAssocDisord* **22**:116-124.

K Miyata NO, H. Uchino, T. Yamaguchi, A. Isshik and F. Shibasaki (2001) Involvement of the brain-derived neurotrophic factor/TrkB pathway in neuroprotective effect of cyclosporin A in forebrain ischemia. *Neuroscience* **105**:571-578.

Kosfeld M, Heinrichs M, Zak PJ, Fischbacher U and Fehr E (2005) Oxytocin increases trust in humans. *Nature* **435**:673-676.

Li X, Elwell MR, Ryan AM and Ochoa R (2003) Morphogenesis of postmortem hepatocyte vacuolation and liver weight increases in Sprague-Dawley rats. *Toxicol Pathol* **31**:682-688.

Liu B, Jiang J-W, Wilson BC, Du L, Yang S-N, Wang J-Y, Wu G-C, Cao X-D and Hong J-S (2000) Systemic Infusion of Naloxone Reduces Degeneration of Rat Substantia Nigral Dopaminergic Neurons Induced by Intranigral Injection of Lipopolysaccharide. *Journal of Pharmacology and Experimental Therapeutics* **295**:125-132.

Lu CT, Zhao YZ, Wong HL, Cai J, Peng L and Tian XQ (2014) Current approaches to enhance CNS delivery of drugs across the brain barriers. *Int J Nanomedicine* **9**:2241-2257.

Lux J and Sherry AD (2018) Advances in gadolinium-based MRI contrast agent designs for monitoring biological processes in vivo. *Current Opinion in Chemical Biology* **45**:121-130.

McGeer PL and McGeer EG (1995) The inflammatory response system of brain: implications for therapy of Alzheimer and other neurodegenerative diseases. *Brain Research Reviews* **21**:195-218.

Mittal D, Ali A, Md S, Baboota S, Sahni JK and Ali J (2014) Insights into direct nose to brain delivery: current status and future perspective. *Drug Deliv* **21**:75-86.

Moore GE and Sandberg AA (1964) Studies of a human tumor cell line with a diploid karyotype. *Cancer* **17**:170-175.

Osman MM, Lulic D, Glover L, Stahl CE, Lau T, van Loveren H and Borlongan CV (2011) Cyclosporine-A as a neuroprotective agent against stroke: its translation from laboratory research to clinical application. *Neuropeptides* **45**:359-368.

Patrick FMGaJW (1996) Neuronal localization of the Cyclophilin A protein in the adults rat brain. *The Journal of Comparative Neurology*:283-293.

Per G Djupesland JCMaRAM (2014) The nasal approach to delivering treatment for brain diseases: an anatomic, physiologic, and delivery technology overview. *Therapeutic Delivery* **5**:709-733.

Sandip T, Yi-Meng T and Mansoor A (2006) Preparation and In vitro Characterization of Multifunctional Nanoemulsions for simultaneous MR Imaging and Targeted Drug Dleivery. *J biomed Nanotech* **2**:217-224.

Schauwecker JBSaPE (2003) Protection Provided by Cyclosporin A against excitotoxic Neuronal death is genotype dependent. *Epilepsia* **44**:995-1002.

Singh Y, Meher JG, Raval K, Khan FA, Chaurasia M, Jain NK and Chourasia MK (2017) Nanoemulsion: Concepts, development and applications in drug delivery. *J Control Release* **252**:28-49.

Solomon H. Snyder DMS, Michael M. Lai, Joseph P. Steriner, Gregory S. Hamilton and Peter D. Suzdak (1998) Neural actions of immunophilin ligands. *Trends in Pharmacological Sicences* **19**:21-26.

Tomás-Camardiel M, Rite I, Herrera AJ, de Pablos RM, Cano J, Machado A and Venero JL (2004) Minocycline reduces the lipopolysaccharide-induced inflammatory reaction, peroxynitrite-mediated nitration of proteins, disruption of the blood–brain barrier, and damage in the nigral dopaminergic system. *Neurobiology of Disease* **16**:190-201.

Wengst A and Reichl S (2010) RPMI 2650 epithelial model and three-dimensional reconstructed human nasal mucosa as in vitro models for nasal permeation studies. *Eur J Pharm Biopharm* **74**:290-297.

Westin U, Piras E, Jansson B, Bergstrom U, Dahlin M, Brittebo E and Bjork E (2005) Transfer of morphine along the olfactory pathway to the central nervous system after nasal administration to rodents. *EurJ PharmSci* **24**:565-573.

Yadav S, Gattacceca F, Panicucci R and Amiji MM (2015) Comparative Biodistribution and Pharmacokinetic Analysis of Cyclosporine-A in the Brain upon Intranasal or Intravenous Administration in an Oil-in-Water Nanoemulsion Formulation. *Mol Pharm* **12**:1523-1533.

Yi X, Manickam DS, Brynskikh A and Kabanov AV (2014) Agile delivery of protein therapeutics to CNS. *J Control Release* **190**:637-663.

FIGURE LEGENDS

Figure 1: A) Cellular transport of cyclosporine in solution (T-CSA), NE-SA (positively charged nanoemulsion) and NE-T (negatively charged nanoemulsion) through RPMI 2650 monolayer cells from apical to basolateral (AB) and basolateral to apical (BA) (data presented as mean ± S.D, n=3) **B)** Intracellular uptake of cyclosporine in solution (T-CSA), NE-SA (positively charged nanoemulsion) and NE-T (negatively charged nanoemulsion) in RPMI 2650 cells at 3 and 24 hrs (data presented as mean ± S.D, n=3). **C)** RPMI 2650 Cell viability results for CSA nanoemulsion formulations (cyclosporine in solution (T-CSA), NE-SA (positively charged nanoemulsion) and NE-T (negatively charged nanoemulsion) at 10 and 20 μM concentration respectively when compared to solution of CSA at 48 hrs. Only media was used as a negative control and treatment with PEI (poly (ethylenemine) was used as a positive control. (Data presented as mean +/- S.D n=8).

Figure 2: Inflammatory marker TNFα, iNOS, IL-1 and IL-6 specific mRNA results showing transcript expression in the J774A.1 macrophage cell line. With LPS treatment (positive control) there was a significant increase in mRNA expression of cytokines Tnf α (** ($p<0.001$), iNOS (* ($P<0.05$), IL-1 (*** ($p<0.0001$) and mIL-6 (* ($p<0.05$). With NE-SA (positively charged CSA nanoemulsion) treatment there was a significant decrease in expression of inflammatory cytokines iNOS (* $p<0.05$), IL-1 (*** ($p<0.001$) and mIL-6 (* ($P<0.05$) as compared to LPS alone treatment. There was a significant decrease in expression of IL-1 (**** ($p<0.0001$) and mIL-6 (* ($p<0.05$) for NE-SA treated group when compared to CSA-S (CSA in solution) treated group. Untreated cells were used a negative control. *The values reported are mean ± SD (n = 3).* All statistics were performed using One-way ANOVA(Tukey's multiple comparison test).

Figure 3: A) Highlighted major brain regions in an anterior to posterior overlay of rat brain atlas showing significant change in T1 values for Nanoemulsion-Gd compared to control or Magnevist® at 25-30 min time point post dose**. B)** Gd^{3+} ion containing nanoemulsion distribution at 25-30 min time point compared to Magnevist and control in major regions of brain. There was a significant % change decrease in T1 values for different brain regions for NE-SA group (* ($p<0.05$), ** ($p<0.001$) as compared to control. **C)** Nanoemulsion-Gd distribution at 55-60 min time point compared to Magnevist and control in major regions of brain There was a significant decrease in T1 values for NE-SA group (* ($p<0.05$) as compared to control .
Statistical student's *t* tests were performed on % change of T1 value for major brain regions and specific 172 brain regions of each subject. The t-test statistics using a 95% confidence level (*$p<0.05$) and 99% (**$p<0.001$) confidence level, 2-tailed distributions, and heteroscedastic variance assumptions were performed.

Figure 4: A) Representative overlay of rats brain regions showing distribution in different specific regions following Intranasal administration of Gd contrast agent containing. **B)** Nanoemulsion-Gd distribution at 25-30 min time point compared to Magnevist and control in specific regions of brain**.** There was a significant decrease in T1 values for NE-SA treated group for different brain region (* ($p<0.05$) as compared to control.
Statistical student's *t* tests were performed on % change of T1 value for major brain regions and specific 172 brain regions of each subject. The t-test statistics using a 95% confidence level (*$p<0.05$) and 99% (**$p<0.001$) confidence level, 2-tailed distributions, and heteroscedastic variance assumptions were performed.

Figure 5: Inflammatory marker TNFα, iNOS, IL-2 and IL-6 specific mRNA results showing transcript expression in the substantia nigra region of rat brain after treating rats with only saline, only LPS, CSA-NE + LPS and CSA-S + LPS. There was a significant decrease in TNF-α expression after treatment with NE-SA (positively charged nanoemulsion) as compared to LPS alone. Saline treated rats were used as negative controls and LPS treated rats were used as positive control. (* $p<0.05$). *The values reported are mean ± SEM (n = 5).*
Statistical analysis was performed using student's t-test for comparison of various groups.

Figure 6: A) Body weight measurements to determine safety/tolerability profile upon single intranasal administration of the control (saline) and positively charged CSA nanoemulsion (NE-CSA). **B)** The values are reported as percent change in body weight as a function of pre-treatment weight of rats. **C)** Histology of nasal respiratory, olfactory epithelium and liver after intranasal dosing of CSA formulations (NE-SA and CSA-S).

Tables:

Table 1. Composition and Characterization Properties of Anionic and Cationic Nanoemulsions Formulations of Cyclosporine-A (CSA).

Formulation	Composition	CSA Initial Loading Conc. (mg/ml)	Hydrodynamic Diameter of Oil Droplet (nm)	Polydispersity Index	Zeta Potential (mV)	Percent CSA Encaps-ulation
CSA-Encapsulated Anionic Nanoemulsion (NE-T)	Lipoid E80, Tween 80 and Flax-seed Oil	25	232±10*	0.25±0.06	-33±12	88±10
CSA-Encapsulated Cationic Nanoemulsion (NE-SA)	Lipoid E80, Tween 80, Stearylamine, and Flax-seed Oil	30	272±12	0.3±0.09	57±10	88±13

*Mean ± S.D. (n = 4)

JPET Fast Forward. Published on December 27, 2018 as DOI: 10.1124/jpet.118.254672
This article has not been copyedited and formatted. The final version may differ from this version.

JPET Fast Forward. Published on December 27, 2018 as DOI: 10.1124/jpet.118.254672
This article has not been copyedited and formatted. The final version may differ from this version.

Figures

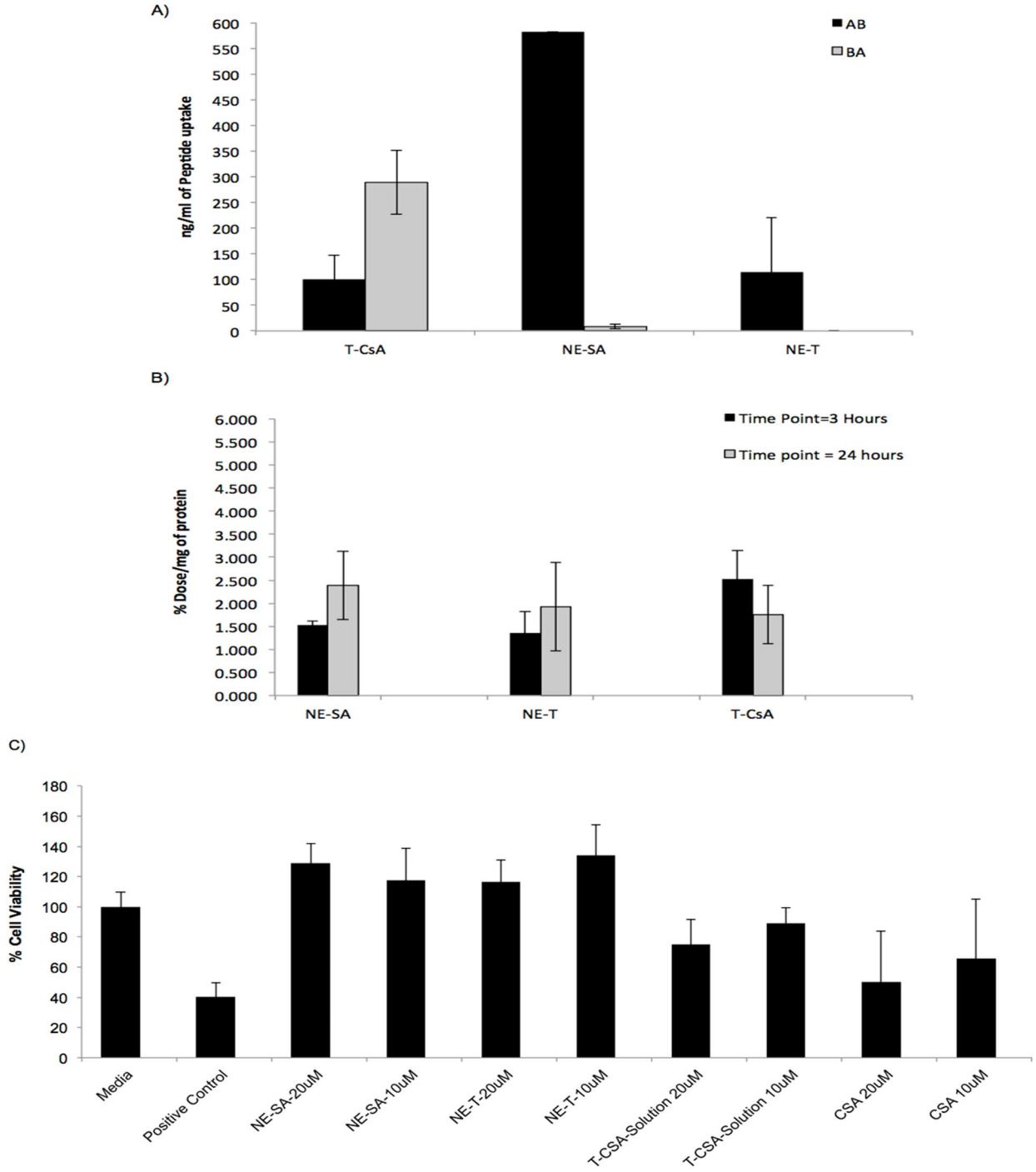

Figure 1

JPET Fast Forward. Published on December 27, 2018 as DOI: 10.1124/jpet.118.254672
This article has not been copyedited and formatted. The final version may differ from this version.

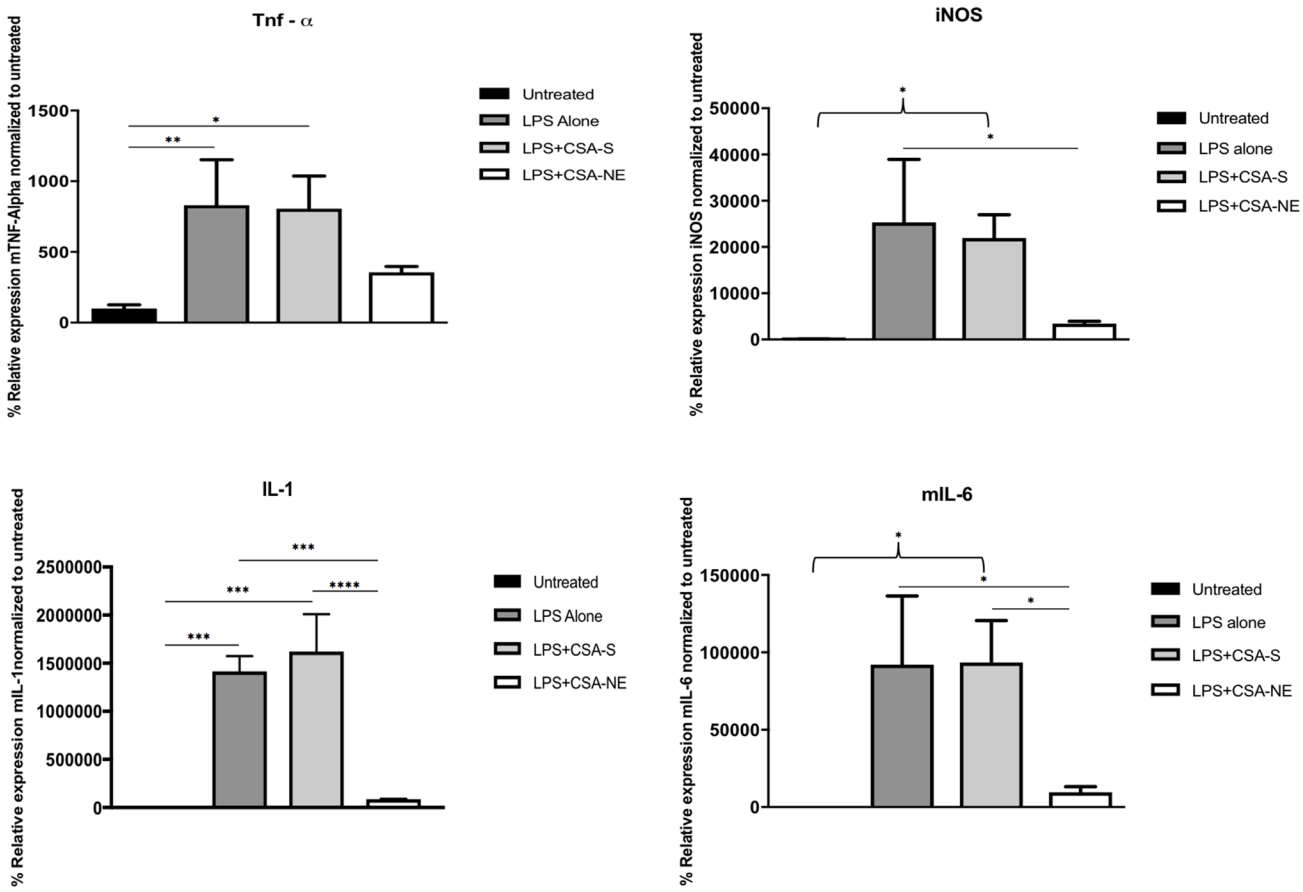

Figure 2.

JPET Fast Forward. Published on December 27, 2018 as DOI: 10.1124/jpet.118.254672
This article has not been copyedited and formatted. The final version may differ from this version.

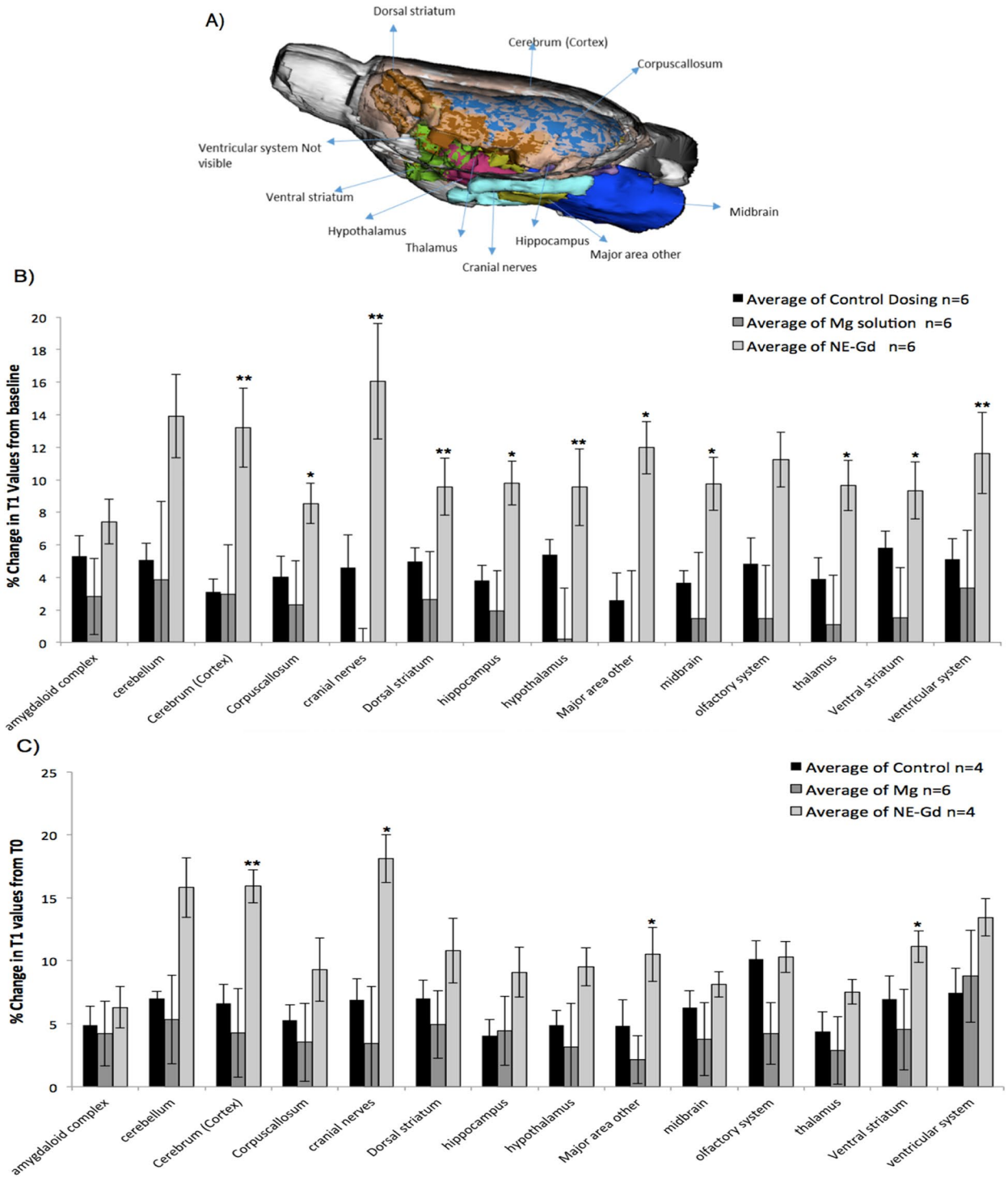

Figure 3.

JPET Fast Forward. Published on December 27, 2018 as DOI: 10.1124/jpet.118.254672
This article has not been copyedited and formatted. The final version may differ from this version.

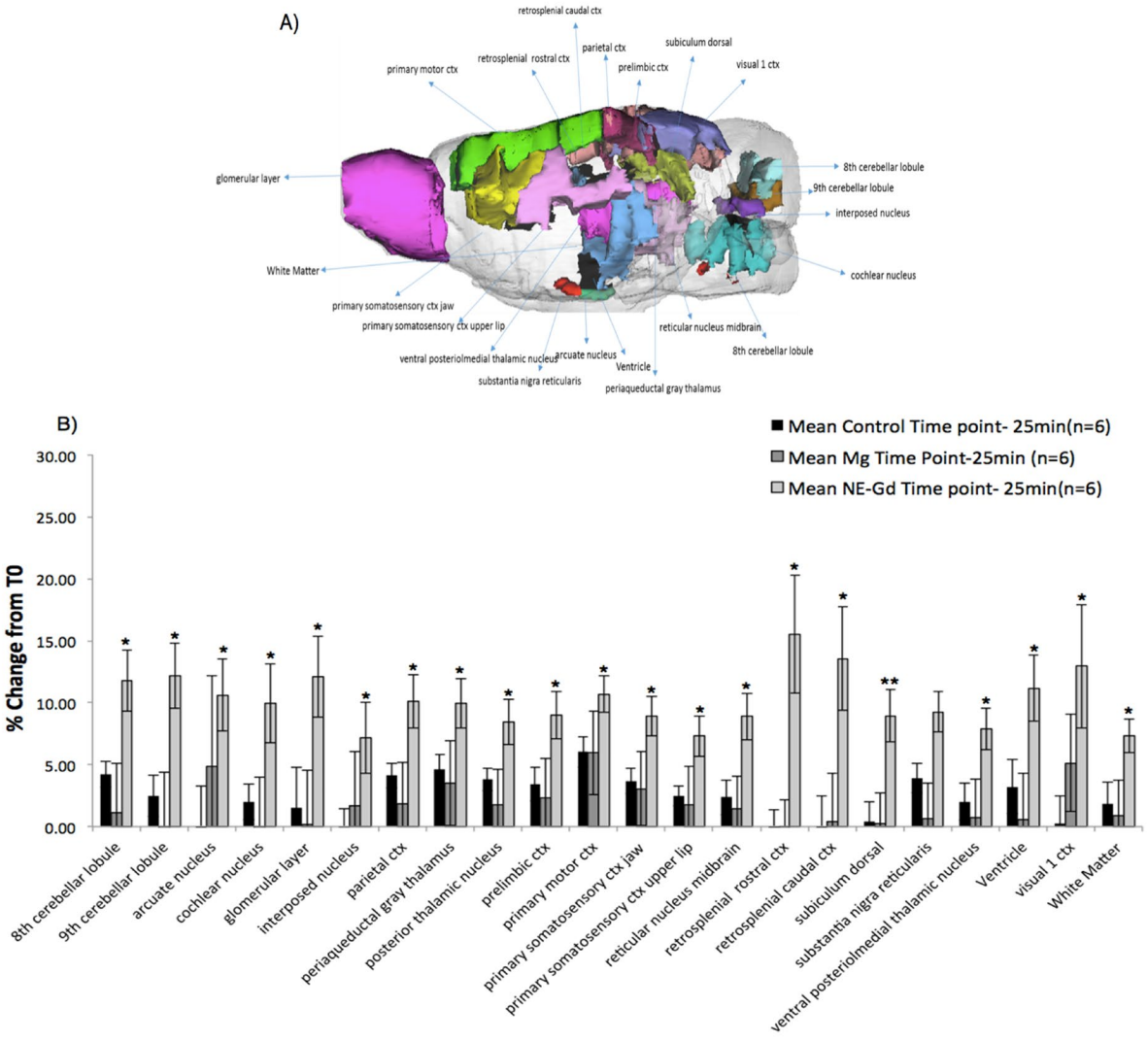

Figure 4.

JPET Fast Forward. Published on December 27, 2018 as DOI: 10.1124/jpet.118.254672
This article has not been copyedited and formatted. The final version may differ from this version.

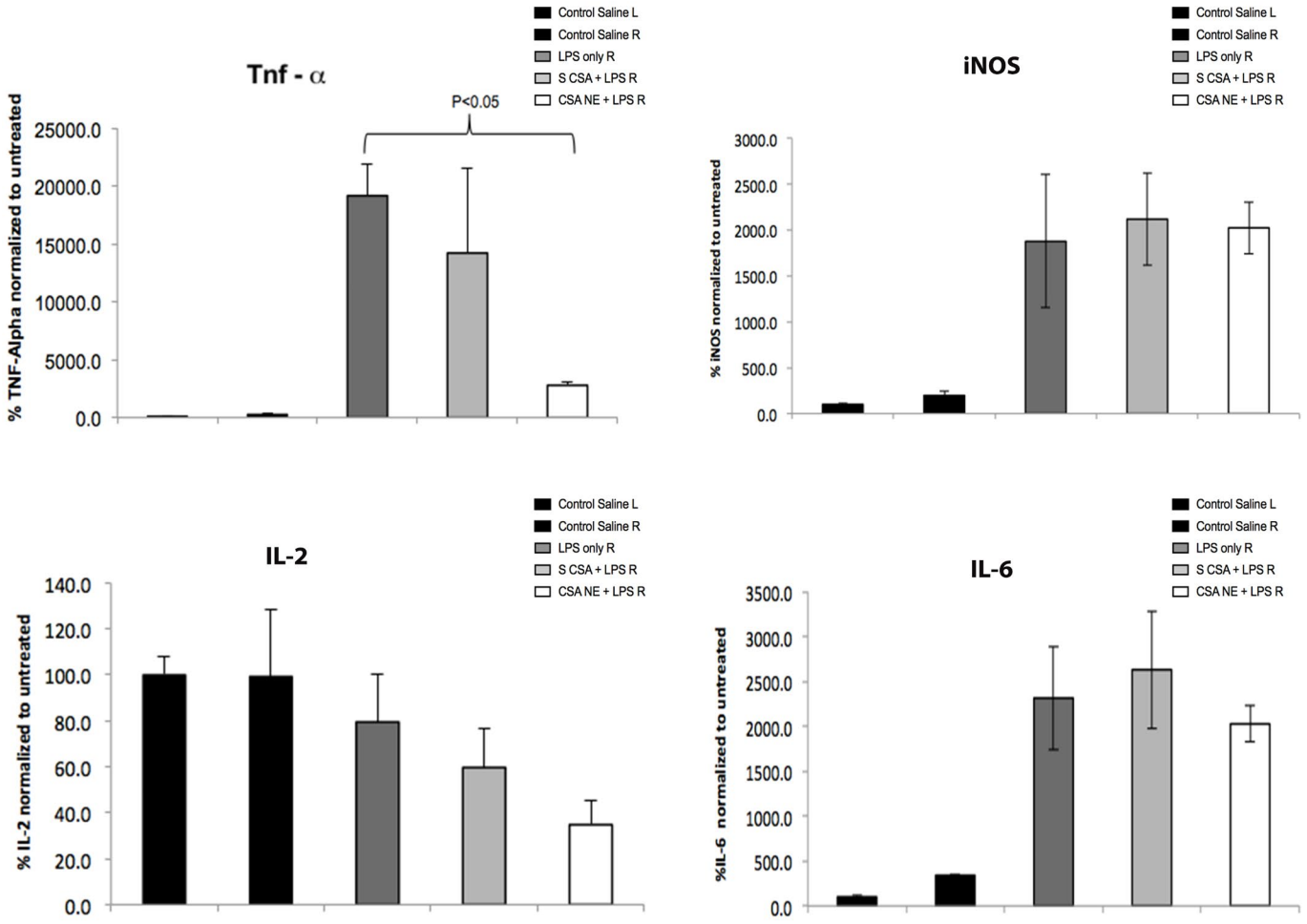

Figure 5.

JPET Fast Forward. Published on December 27, 2018 as DOI: 10.1124/jpet.118.254672
This article has not been copyedited and formatted. The final version may differ from this version.

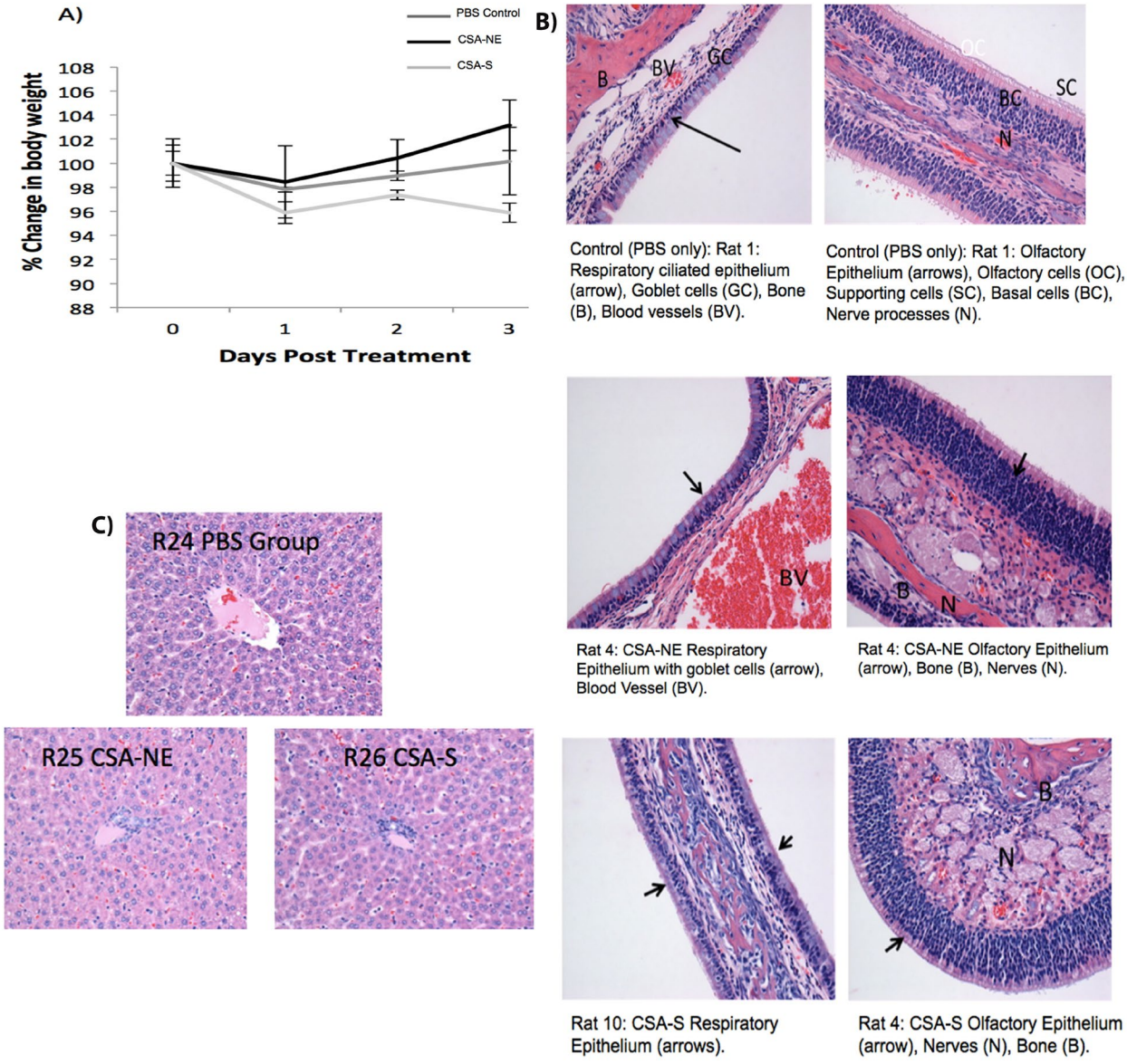

Figure 6.

CNS Delivery and Anti-Inflammatory Effects of Intranasally Administered Cyclosporine-A in Cationic Nanoemulsion Formulations.

Sunita Yadav[1,3], Grishma Pawar[1], Praveen Kulkarni[2], Craig Ferris[1,2], and Mansoor Amiji[1,4]

[1]Department of Pharmaceutical Sciences, School of Pharmacy
Northeastern University, Boston, MA 02115 USA
[2]Center for Translational Neuro-Imaging, Northeastern University,
Boston, MA 02115 USA
[3]Novartis Institute of Biomedical Research, Cambridge, MA 02142 USA

Journal Title – The Journal of Pharmacology and Experimental Therapeutics

13. Supplementary figures

Formulation	Composition	CsA Initial Loading Conc. (mg/ml)	Hydrodynamic Diameter of Oil Droplet (nm)	Polydispersity Index	Zeta Potential (mV)	Percent CsA Encapsulation
CsA-Encapsulated Anionic Nanoemulsion (NE-T)	Lipoid E80, Tween 80 and Flax-seed Oil	25	232±10*	0.25±0.06	-33±12	88±10
CsA-Encapsulated Cationic Nanoemulsion (NE-SA)	Lipoid E80, Tween 80, Stearylamine, and Flax-seed Oil	30	272±12	0.3±0.09	57±10	88±13

Table 1: Composition and characterization properties of Anionic (NE-T) and Cationic (NE-SA) Nanoemulsion formulation of Cyclosporine-A (CsA).

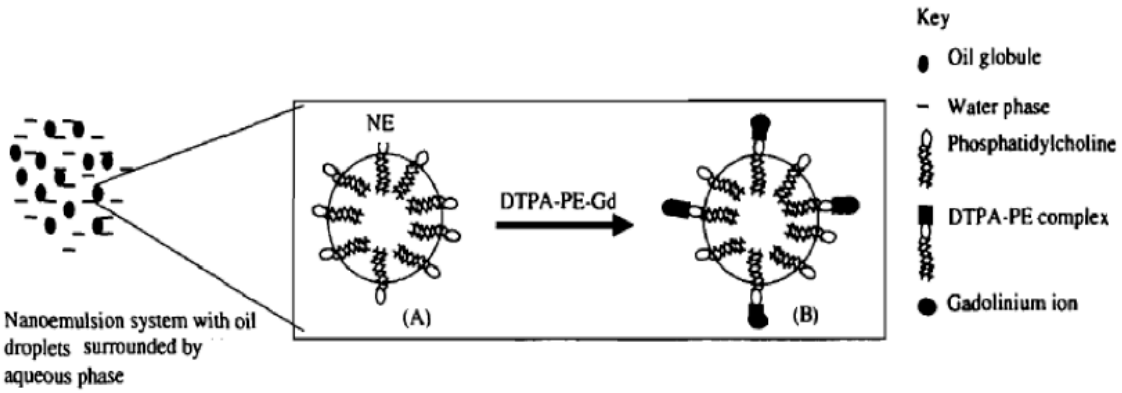

Supplementary figure 1: Schematic representation of a nanoemulsion (NE) complexed with DTPA-PE-Gd3+. *A: Surface arrangement of phosphatidylcholine molecules with lipophilic tail embedded within the oily droplet while polar head groups positioning on the interface of the oil and water phase. B: Association of DTPA-PE-Gd3+ molecules with the oily droplet in analogous manner to phosphatidylcholine*

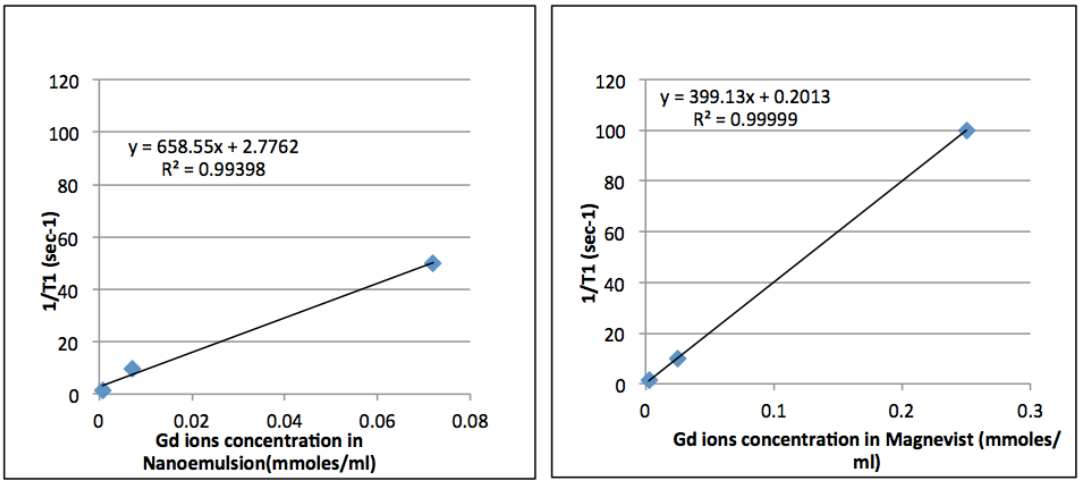

Supplementary Figure 2: *In vitro* MRI (Magnetic Resonance Imgaing) relaxation rate plot of NE (nanoemulsion) and Magnevist (R1= 1/T1) as function of concentration of DTPA-PE-Gd3+.

A B C

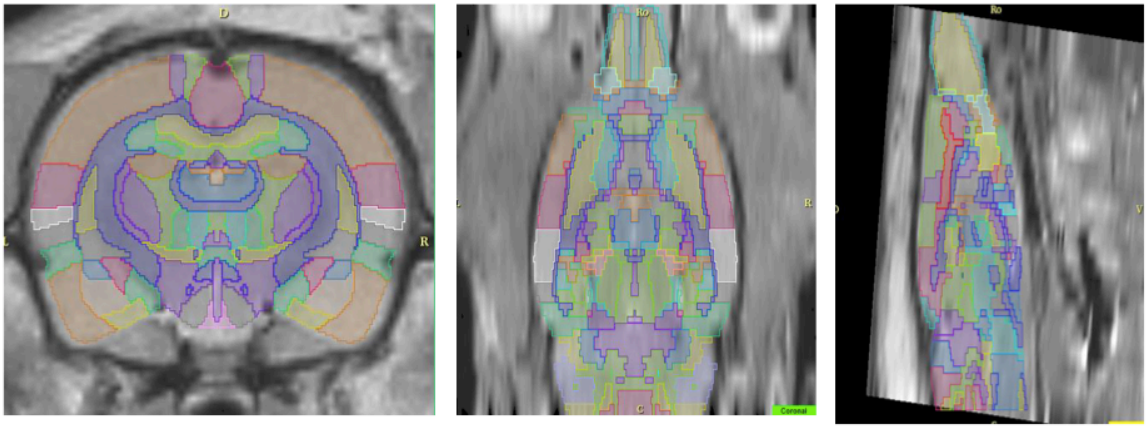

Supplementary Figure 3 (a) Brain atlas overlays of axial registration, (b) coronal view segmentation and (c) sagittal view segmentation